AD-A063 400 NAVAL OCEAN SYSTEMS CENTER SAN DIEGO CA F/G 9/3
DETECTION OF SINUSOIDS IN WHITE NOISE USING ADAPTIVE LINEAR PRE--ETC(U)
MAY 78 S T ALEXANDER, R MEDAUGH, M SHENSA N00123-76-C-1937
UNCLASSIFIED NOSC/TR-270 NL

| OF |
AD A063400

END
DATE FILMED
3-79
DDC

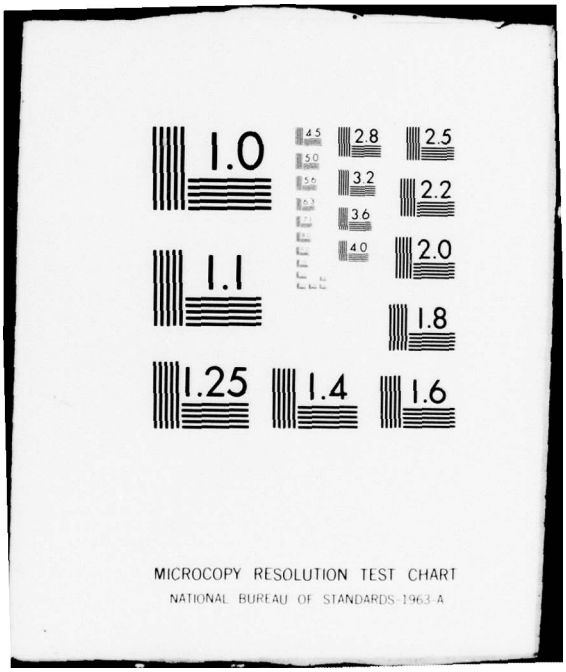
1.0
1.1
1.25
1.4
1.6
1.8
2.0
2.2
2.5
2.8
3.2
3.6
4.0
4.5
5.0
MICROCOPY RESOLUTION TEST CHART
NATIONAL BUREAU OF STANDARDS-1963-A

NOSC

NOSC TR 270

Technical Report 270

DETECTION OF SINUSOIDS IN WHITE NOISE USING ADAPTIVE LINEAR PREDICTION FILTERING

ST Alexander, JR Zeidler (NOSC)
R Medaugh (University of Colorado)
M Shensa (Hydrotronics, Inc)

1 May 1978

Research and Development: October 1977 - May 1978

Prepared for
Naval Electronic Systems Command

Approved for public release; distribution unlimited.

NAVAL OCEAN SYSTEMS CENTER
SAN DIEGO, CALIFORNIA 92152

NAVAL OCEAN SYSTEMS CENTER, SAN DIEGO, CA 92152

AN ACTIVITY OF THE NAVAL MATERIAL COMMAND

RR GAVAZZI, CAPT, USN
Commander

HL BLOOD
Technical Director

ADMINISTRATIVE INFORMATION

This work was sponsored by the Naval Electronic Systems Command (Code 320) under program element 62711N, task area XF11-121, and performed during fiscal year 1978. M Shensa is with Hydrotronics, Inc., San Diego, California, and R Medaugh is with the Univeristy of Colorado, Boulder. Their participation was supported under contracts N00123-76-C-1937 and N00953-77-C-008 respectively.

Released by
RH HEARN, Head
Electronics Division

Under authority of
DA KUNZ, Head
Fleet Engineering Department

(9) Technical rept. Oct 77-May 78,

UNCLASSIFIED

SECURITY CLASSIFICATION OF THIS PAGE *(When Data Entered)*

REPORT DOCUMENTATION PAGE

READ INSTRUCTIONS BEFORE COMPLETING FORM

(14) 1. REPORT NUMBER: NOSC/TR-270

2. GOVT ACCESSION NO.

3. RECIPIENT'S CATALOG NUMBER

(6) 4. TITLE *(and Subtitle)*: DETECTION OF SINUSOIDS IN WHITE NOISE USING ADAPTIVE LINEAR PREDICTION FILTERING.

(1) 5. TYPE OF REPORT & PERIOD COVERED: Research and Development, October 1977-May 1978

6. PERFORMING ORG. REPORT NUMBER

7. AUTHOR(s)

ST Alexander, R Medaugh, M Shensa, JR Zeidler

8. CONTRACT OR GRANT NUMBER(s): N00123-76-C-1937, N00953-77-C-008

9. PERFORMING ORGANIZATION NAME AND ADDRESS

Naval Ocean Systems Center
San Diego, California 92152

10. PROGRAM ELEMENT, PROJECT, TASK AREA & WORK UNIT NUMBERS

62711N, XF11-121

11. CONTROLLING OFFICE NAME AND ADDRESS

Naval Electronic Systems Command
Washington, DC

(11) 12. REPORT DATE: 1 May 1978

13. NUMBER OF PAGES: 30 (12) 32

14. MONITORING AGENCY NAME & ADDRESS *(if different from Controlling Office)*

(10) S. T. /Alexander, R. /Medaugh
M. /Shensa J. R. /Zeidler

15. SECURITY CLASS. *(of this report)*: UNCLASSIFIED

15a. DECLASSIFICATION/DOWNGRADING SCHEDULE

16. DISTRIBUTION STATEMENT *(of this Report)*

Approved for public release; distribution unlimited.

(15) N00123-76-C-1937, N00953-77-C-0008

17. DISTRIBUTION STATEMENT *(of the abstract entered in Block 20, if different from Report)*

(16) F11121

18. SUPPLEMENTARY NOTES

19. KEY WORDS *(Continue on reverse side if necessary and identify by block number)*

Adaptive line enhancing

Detection theory

Adaptive filtering

20. ABSTRACT *(Continue on reverse side if necessary and identify by block number)*

This paper analyzes the detection performance of a data-adaptive detector based on an adaptive linear prediction (ALP) filter incorporating the Widrow-Hoff LMS algorithm. Receiver operating characteristic (ROC) curves are calculated for two distinct adaptive detector implementations for the case of a sinusoid of known frequency but unknown phase embedded in white Gaussian additive noise. Comparative performance curves for adaptive and nonadaptive detector implementations are presented for this classical detection problem. The dependence of detection performance on the frequency resolution and time constant of the adaptive filter is treated. The ROC curves of the adaptive detector are derived for the condition that the ALP filter output statistics are Gaussian and that the magnitude square output has chi-square density with two degrees of freedom.

DD FORM 1 JAN 73 1473 EDITION OF 1 NOV 65 IS OBSOLETE
S/N 0102-LF-014-6601

UNCLASSIFIED

SECURITY CLASSIFICATION OF THIS PAGE *(When Data Entered)*

393 159

JOB

CONTENTS

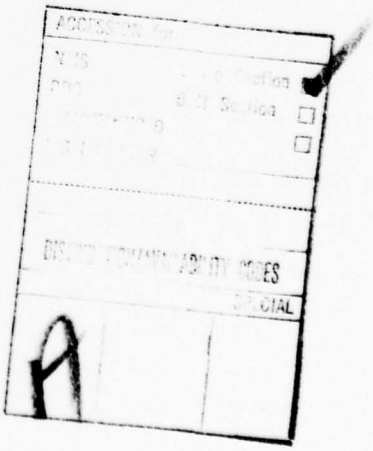

INTRODUCTION

Several types of data adaptive detection structures* have been proposed for use in environments where the signal and noise statistics are only vaguely known and where insufficient a priori information is available to design optimal detectors. Adaptive mean level detectors have been implemented to provide improved performance over conventional nonadaptive systems when the noise statistics are nonstationary (ref. 1-7). Other forms of adaptive receivers based on pattern recognition techniques, decision-directed feedback, nonparametric statistics, and sequential processing are described in references 8–14. Adaptive implementations of linear prediction filters have also been proposed for spectral analysis, instantaneous frequency estimation, data compression, adaptive deconvolution, system identification, adaptive noise suppression, and speech encoding applications (ref 15–29). The computational simplicity of adaptive linear prediction (ALP) implementations based on the Widrow-Hoff least-mean-squares (LMS) adaptive algorithm is discussed in references 16,18,20.

Several recent papers (ref. 17,21–25) have been concerned with the use of adaptive linear prediction filters as self-tuning filters for the detection of narrowband signals in noise. In the present study an L-weight ALP filter is used to estimate the frequencies at which coherent energy is present in the input data sequence, and a K-point spectrum analyzer is used to examine either the transfer function of the adaptive filter weights or the power spectrum of the adaptive filter output, as illustrated in figure 1. Appropriate selection of the prediction distance (Δ in figure 1) on the basis of available a priori information concerning the expected autocorrelation of the noise and signal components allows the ALP filter to suppress either the correlated or uncorrelated noise components of the input data. This device, pictured in figure 2, has been called an "adaptive line enhancer" (ALE) due to the narrowband signal enhancement which results from the broadband noise suppression capability of a linear prediction filter (ref. 17).

The purpose of this paper is to analyze ALE detection performance on the basis of reciever operating characteristic (ROC) curves for inputs consisting of a sinusoidal signal of known frequency but unknown phase embedded in white Gaussian additive noise of known power. This is the classical signal-known-except-for-phase (SKEP) detection problem for which the optimal detector is well known (14,30,31). When the available observation interval is long, however it is often impractical to implement the optimal detector; thus, practical spectrum analyzers typically employ incoherent averaging to minimize hardware requirements. For completeness, the performance curves obtained for the adaptive detector are compared with those of both the optimal detector and a commonly used nonadaptive detector illustrated in figure 3.

It is generally possible to design a nonadaptive detector which is superior to an adaptive detector in a stationary operating environment. However, adaptive detectors can prove advantageous in nonstationary operating environments (ref. 1–7,24). A goal of this paper is to provide baseline performance criteria to aid in selecting appropriate ALE time constants, filter lengths, and other design parameters for narrowband detection applications where the SKEP detection problem represents an appropriate analytical model for

*An adaptive detection system is one in which the detector structure is based to some extent on the received data and which incorporates a mechanism to vary the detector structure as the received signal and noise characteristics evolve in time.

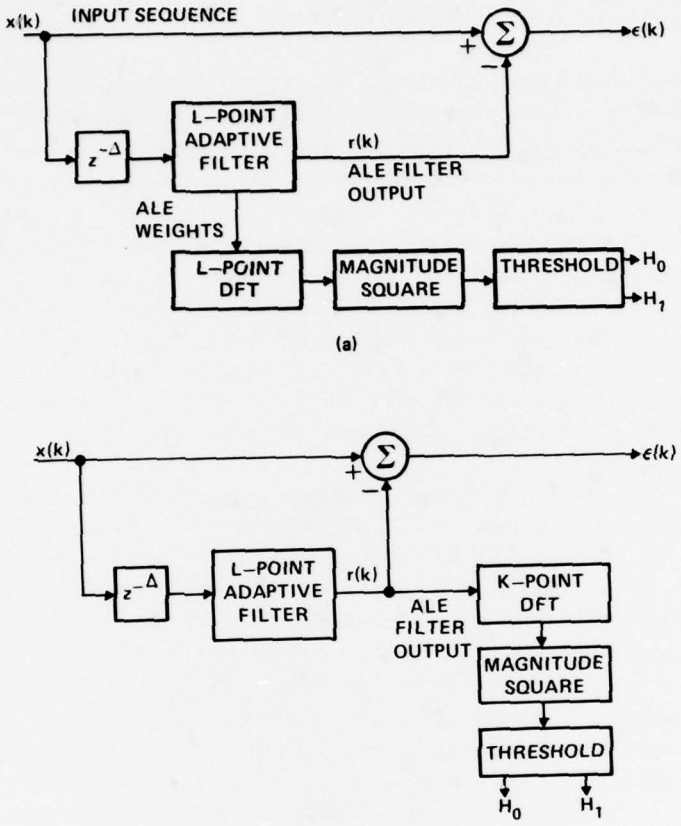

Figure 1. Adaptive detector implementations. (a) ALE weight transform. (b) ALE output transform.

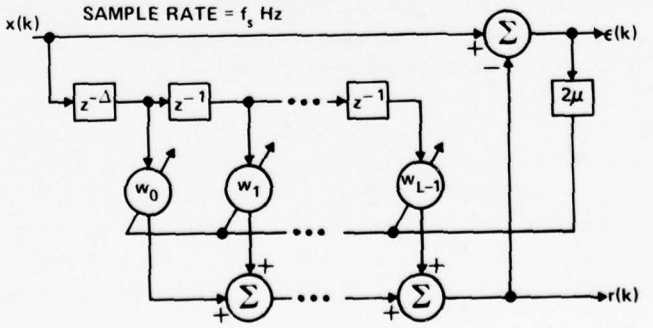

Figure 2. Block diagram of adaptive line enhancer.

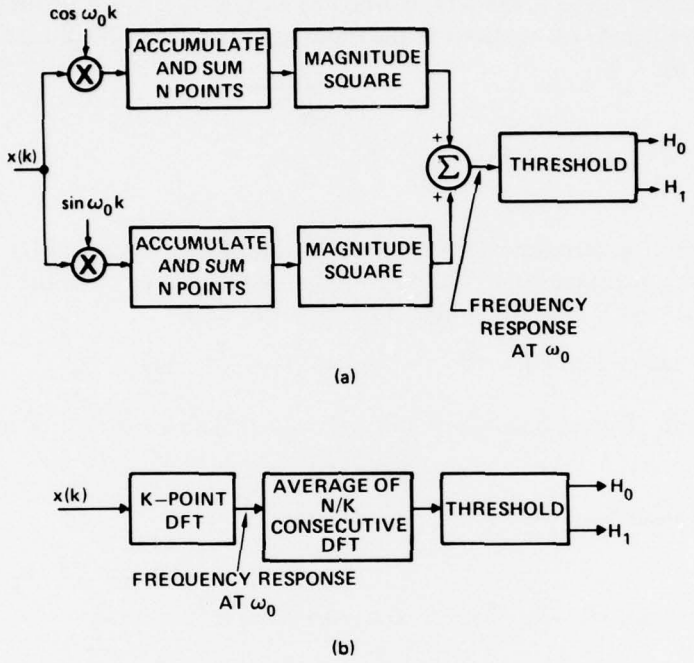

Figure 3. Processor structures for coherent DFT and incoherently averaged detector. (a) Coherent DFT. (b) Incoherently averaged detector.

the input signal and noise conditions in which the detector may operate. These results in turn allow the sensitivity in performance to be determined as a function of the adaptive filter parameters.

The Widrow-Hoff LMS algorithm provides a computationally efficient method for updating the ALP filter coefficients to track temporal variations in the signal and noise statistics (ref. 16–20). All performance analyses of the ALE in this paper are based on an ALP filter which is updated by this algorithm (figure 2).

In suceeding sections, the sensitivity of the ALE detector to the feedback parameter μ is investigated and found to be relatively small. It is further shown that, for L = K, the detection performance of the two adaptive detectors in figure 1 compares favorably with that of N/K independent incoherent averages of a K-point DFT (figure 3), provided N, the length of the data sequence is of the order of the ALE convergence time. Finally, a study is made of the effects of varying K.

ADAPTIVE WEIGHT VECTOR MODEL

As illustrated in figure 1, the ALE consists of an L-weight linear prediction filter in which the filter coefficients are updated at the input sampling rate. The adaptive filter output r(k) is defined by

$$r(k) = \sum_{j=0}^{L-1} w_j(k)x(k - j - \Delta) \quad , \tag{1}$$

where Δ is the prediction distance of the filter. The output r(k) is then subtracted from x(k) to form an error sequence $\epsilon(k)$. The error sequence is fed back to adjust the filter weights according to the Widrow-Hoff LMS algorithm (ref. 30),

$$w_i(k + 1) = w_i(k) + 2\mu\, \epsilon(k)\, x(k - i - \Delta),\ i = 0,1, \ldots, L-1 \quad , \tag{2}$$

where μ is a constant. The ALE weight vector w(k + 1) at time k + 1 may be written from (2) as

$$\underline{w}(k + 1) = \underline{w}(k) + 2\mu\ \underline{x}(k)\, [x(k) - \underline{x}^T(k)\, \underline{w}(k)] \tag{3}$$

where

$$\underline{x}(k) = [x(k - \Delta), x(k - \Delta - 1), \ldots, x(k - \Delta - L + 1)]^T$$

and

$$\underline{w}(k) = [w_0(k), w_1(k), \ldots, w_{L-1}(k)]^T \quad .$$

Taking the expectation of both sides of (3), we have

$$E\{w(k + 1)\} = E\{w(k)\} + 2\mu[E\{x(k)\, x(k)\} - E\{\underline{x}(k)\, \underline{x}^T(k)\, w(k)\}] \quad . \tag{4}$$

Since $E[\underline{w}(k + 1)]$ depends on all the past data x(k), x(k – 1), . . ., computation of the convergence of w(k) in the mean becomes intractable unless some simplifying assumptions are made. For small μ and low input signal-to-noise ratio (SNR), there is very little statistical dependence between the $\underline{x}(k)$ and $\underline{w}(k)$, i.e.,

$$E[\underline{x}^T(k)\, \underline{w}(k)] \cong E[(x^T(k)]\ E[\underline{w}(k)] \quad ,$$

and (5)

$$E\{\underline{x}(k)\, \underline{x}^T(k)\, \underline{w}(k)\} \cong E\{\underline{x}(k)\, \underline{x}^T(k)\}\, E\{w(k)\} \quad .$$

Widrow (ref. 30,17) has shown that, for uncorrelated data, E{w(k)} converges from an arbitrary initial value to w* as $k \to \infty$, provided $0 < \mu < \lambda_{max}^{-1}$, where λ_{max} is the largest eigenvalue of the data autocorrelation matrix and w* is the optimal Wiener filter weight vector. The term w* can be obtained from the solution to the discrete Wiener-Hopf matrix equation,

$$Rw^* = P \quad , \tag{6}$$

where R is the L × L autocorrelation matrix of the input sequence x(k) and P is the L-element cross-correlation vector with elements $P_j = E\{x(k)\, x(k + j + \Delta - 1)\}$. The convergence of the mean weight vector in the more general cases of correlated data and for nonstationary inputs has been considered for both ideal filters and for cases in whch implementation errors are present. It is shown that the convergence properties of the filters are robust under a wide range of conditions, providing that the inputs to the filter satisfy specified nondegeneracy conditions (ref. 33–34). Experimental measurements of the mean weight vector of a hardware implementation of the ALE also confirm that $E\{w(k)\} \rightarrow w^*$ for increasing k for sinusoidal inputs in uncorreclated noise for many cases of interest (ref. 23).

Since the LMS algorithm only approximates the true LMS error gradient, the weight vector coefficients are obtained from noisy estimates of the optimal Wiener filter solution. This gradient estimation noise, often called "misadjustment noise" (ref. 17), is given by

$$V_j(k) = w_j(k) - w_j^* \quad . \tag{7}$$

Widrow et al. (ref. 17) have shown that the variance of V_j may be made arbitrarily small by decreasing the feedback parameter μ. Decreasing μ also increases the convergence time of the LMS algorithm, however, and a compromise between the response time and the misadjustment noise power must be made in practical applications.

It is generally assumed (ref. 17) that the misadjustment noise has a Gaussian distribution. It then follows from (5) that

$$\begin{aligned} &E[V_j(k)] = 0 \quad , \\ &E[V_j(k)V_i(k)] = \mu\xi_{min}\delta(i - j) \quad , \end{aligned} \tag{8}$$

where $\delta(\cdot)$ is the Kronecker delta operator and ξ_{min} is the minimum mean square error power. Analytical solutions for w_j^* for multiple sinusoids in uncorrelated noise have been derived (ref. 23). When

$$x(k) = A \sin(\omega_0 k + \theta) + n(k) \quad , \tag{9}$$

where n(k) is a zero-mean white Gaussian noise sequence of variance υ^2, and ω_0 is known a priori, the sampling frequency can be adjusted so that

$$\frac{\omega_0 L}{2\pi} = \text{integer} \quad , \tag{10}$$

where ω_0 is normalized relative to the sampling frequency of 2π radians. In this case the R-matrix is circulant, and it can readily be shown (ref. 21,23) that

$$w_j^* = \frac{2a^*}{L} \cos[\omega_0(j + \Delta)], \; 0 \leqslant j \leqslant L - 1 \quad , \tag{11}$$

where

$$a^* = \frac{(L/2)\,SNR}{1 + (L/2)\,SNR} \quad , \tag{12}$$

and the input SNR is defined by

$$SNR = A^2/2\upsilon^2 \quad . \tag{13}$$

The amplitude of w_j^* depends nonlinearly on the input SNR, since the transversal filter cannot discriminate between the sinusoid and the broadband noise within the filter passband. It has been shown (ref. 23) that (11) also provides an excellent approximation to w_j^* for $(\pi/L) < \omega_0 < \pi\ [L - 1/(L)]$ for noncirculant autocorrelation matrices.

The speed of adaptation of the LMS algorithm is controlled by the dominant eigenvalues of the R-matrix (ref. 21,34). For the case of a single sinusoid in uncorrelated noise, the optimal weight vector is orthogonal to all eigenvectors of R except the conjugate pair corresponding to frequency ω_0. The eigenvalues associated with these eigenvectors dominate the convergence time and are both approximately given (ref. 21) by

$$\lambda = \upsilon^2 + (A^2L/4) \quad . \tag{14}$$

When the filter is filled with data and all weights are zeroed at k = 0, the mean value $\bar{w}_j(k)$ of the jth weight is updated according to the relation

$$\bar{w}_j(k) = [1 - (1 - 2\mu\lambda)^k]\ w_j^*, \qquad k = 0,1, \ldots \tag{15}$$

For $2\mu\lambda << 1$ and $k >> 1$, (15) is approximated by

$$\bar{w}_j(k) = [1 - e^{-2\mu k\lambda}]\ w_j^*$$

$$= \frac{2a(k)}{L} \cos[\omega_0(j + \Delta)], \quad 0 \leq j \leq L - 1 \quad , \tag{16}$$

where

$$a(k) = [1 - e^{-k/\tau_m}]a^* \quad . \tag{17}$$

In (17), $\tau_m = 1/2\mu\lambda$, the mean adaptation time constant.

It was shown (ref. 35) that the power spectral density of the ALE output for an input consisting of a sinusoid in white noise contains three distinct spectral components: a sinusoidal term due to the filtering of the input sinusoid, a white noise term due to the misadjustment noise, and a narrowband noise term due to the white noise passed through the converged Wiener filter. The relative magnitudes of these components were derived in reference 35. It was further shown that

$$\xi_{min} = \upsilon^2 + (1 - a^*)\ A^2/2 \cong \upsilon^2 \quad . \tag{18}$$

We now derive the detection performance of the two distinct implementations of the ALE illustrated in figure 1. ROC curves are obtained under the condition that the adaptive filter weights are initialized to zero at k = 0, and that N data points are processed prior to forming a detection statistic. The L-weight adaptive filter and the K-point DFT are restricted so that K and L are much less than N. This restriction eliminates the initial transient behavior as the filter fills with data and permits the mean weight approximation (16). In all cases $\Delta = 1$.

DETECTION STATISTICS OF ALE OUTPUT DETECTOR

The ALE output detector is shown in figure 1(b). Detection is based on a K-point DFT of the final K output values from the L-length filter using the classical Neyman-Pearson hypothesis test. Define the two hypotheses, H_0 and H_1, by H_0 : x(k) = n(k) and H_1: x(k) = s(k | θ) + n(k), where s(k | θ) is the sinusoidal signal of known amplitude and frequency but unknown phase and n(k) is a sample of the Gaussian uncorrelated noise sequence with zero mean and variance v^2; i.e.,

$$s(k \mid \theta) = A \sin(\omega_0 k + \theta) \quad , \tag{19}$$

and

$$E[n(k)n(p)] = v^2 \delta(k - p) \quad , \tag{20}$$

where A, ω_0, and v^2 are known a priori and θ is unknown.

Since s(k | θ) is zero-mean, the variable x(k) is a zero-mean Gaussian random variable for all values of k. Thus the filter output r(k | θ) conditioned on the unknown initial phase defined by (1) is a linear combination of products of independent Gaussian variables. It will be assumed that for large L, r(k | θ) is approximately Gaussian. The output spectrum obtained from a K-point DFT of r(k| θ) evaluated at ω_0 is given by $R(\omega_0)$ = u + jv, where $j = \sqrt{-1}$ and

$$u = \sum_{k=0}^{K-1} r(k \mid \theta) \cos \omega_0 k \quad ,$$

$$v = \sum_{k=0}^{K-1} r(k \mid \theta) \sin \omega_0 k \quad . \tag{21}$$

The detection statistic q is then defined as

$$q = u^2 + v^2 \quad . \tag{22}$$

The joint probability density function (PDF) for (u,v) must therefore be specified in order to define the PDF of the detection statistic q. It is shown in the appendix that u and v are essentially statistically independent for the given signal and noise models above. Since r(k | θ) is assumed Gaussian, u and v are also Gaussian and the PDF p(u,v) may be written as

$$p(u,v) = [2\pi\sigma_u\sigma_v]^{-1} \exp\left\{ -\frac{1}{2}\left[\left(\frac{u - \bar{u}}{\sigma_u}\right)^{-2} + \left(\frac{v - \bar{v}}{\sigma_v}\right)^{-2}\right]\right\} , \tag{23}$$

where $\bar{u}$ and $\bar{v}$ are the component means and σ_u^2 and σ_v^2 their variances.

Expressions for $\bar{u}$, $\bar{v}$, σ_u^2, and σ_v^2 are derived in the appendix and appear in equations (A.9), (A.10), (A.52), and (A.53), with the attendent restriction that $(\pi/M) << \omega_0 << \pi - (\pi/M)$, where M = min (K,L). (See references 36 and 37 for additional detail.) Provided that $N > \tau_m$ and that (L,K) << N, a^* in (A.9), (A.10), and (A.52) can be approximated by a(k), as defined by (17), to describe the output statistics just prior to convergence. Thus, under H_1:

$$\bar{u} = A \sin\theta \, ; \, \bar{v} = A \cos\theta \quad , \tag{24}$$

where

$$\tilde{A} = a(k)\, AK/2. \tag{25}$$

In addition, the variance under H_1, σ_1^2, can be expressed as

$$\sigma_1^2 = \sigma_u^2 = \sigma_v^2 = \frac{\mu\xi_{min} v^2 LK}{2} + \frac{\mu\xi_{min} A^2 LK^2}{8} + \frac{2a^2(k) v^2 D}{L^2} \quad , \tag{26}$$

where

$$D = \begin{cases} \frac{K^2 L}{4} - \frac{K^3}{12} \quad , \quad K \leqslant L \quad , \\ \frac{L^2 K}{4} - \frac{L^3}{12} \quad , \quad K > L \quad . \end{cases}$$

The first two components of σ_1^2 are independent of the time index because of the assumption that the weight misadjustment noise is independent of k in (8). The first term in (26) is due to the broadband weight misadjustment noise produced by the input white noise. The second component of σ_1^2 arises from a narrowband noise process centered at frequency ω_0 due to the weight misadjustment caused by the signal. This narrowband noise process may be intrepreted as a random-amplitude sinusoid with frequency ω_0. The third component of the variance arises from the white noise passed by the adaptive filter and increases in magnitude with increasing k. Under H_0, a(k) = 0, and the component means and variances defined by (24-26) reduce to $\bar{u} = \bar{v} = 0$ and

$$\sigma_0^2 = \frac{\mu\xi_{min} v^2 LK}{2} \quad . \tag{27}$$

The derivation of the probability density function for the detection variable q defined by (22) is straightforward (ref. 14,30). It is readily shown that, under H_0, $p_0(q)$ is the gamma density function with two degrees of freedom given by

$$p_0(q) = \frac{1}{2\sigma_0^2} \exp\left[-q/2\sigma_0^2\right] \quad , \quad q \geqslant 0 \quad . \tag{28}$$

Under H_1, q has a density function $p_1(q)$ given by

$$p_1(q) = \frac{1}{2\sigma_1^2} \exp\left[-\frac{1}{2\sigma_1^2}(q + \tilde{A}^2)\right] I_0\left(\frac{Aq^{1/2}}{2\sigma_1^2}\right) \quad , \quad q \geqslant 0 \quad , \tag{29}$$

where $I_0(x)$ is the modified Bessel function of the first kind.

According to the Neyman-Pearson criteria, the probability of false alarm P_{FA} determines the threshold β_0 under H_0:

$$P_{FA} = \int_{q=\beta_0}^{\infty} p_0(q)dq \quad . \tag{30}$$

Since P_{FA} and $p_0(q)$ are known, (3) completely specifies the threshold β_0. When the signal is present, the probability of detection P_D is given by

$$P_D = \int_{q=\beta_0}^{\infty} p_1(q)dq \quad . \tag{31}$$

Through a change of variables it may be shown (ref. 30) that equivalent forms of these integrals are

$$P_{FA} = \int_{p=T_0}^{\infty} \chi_2^2(p)dp \tag{32}$$

and

$$P_D = \int_{p=T_1}^{\infty} \chi_2^{2'}(p \mid \alpha)\, dp \quad , \tag{33}$$

where $\chi_2^2(p)$ is the chi-square PDF with 2 degrees of freedom and $\chi_2^{2'}(p \mid \alpha)$ is the non-centrality parameter α, with

$$\alpha = \tilde{A}^2/\sigma_1^2 = \frac{K^2 a^2(k)\, SNR}{L\,\mu\xi_{min}\left[K + \dfrac{K^2\, SNR}{2} + \dfrac{4a^2(k)\, D}{\mu\xi_{min} L^3}\right]} \tag{34}$$

Specification of P_{FA} in (30) determines the threshold T_0. This threshold is then scaled by the ratio of the variances under H_0 and H_1 to obtain the threshold T_1

$$T_1 = (\sigma_0/\sigma_1)^2\, T_0 = \left[1 + \frac{K}{2} SNR + \frac{4a^2(k)\, D}{\mu\xi_{min} L^3 K}\right]^{-1} T_0 \quad . \tag{35}$$

The probability integrals (30, 31) may be evaluated by a nonnumerical method developed by Urkowitz (ref. 38) or by standard techniques for evaluating Marcum Q-functions or incomplete Toronto functions.

DETECTION STATISTICS OF THE ALE WEIGHT VECTOR IMPLEMENTATION

Reeves (ref. 39) has derived ROC curves for the SKEP detection problem using the ALE weight vector implementation illustrated in figure 1(a). Reeves bases detection on a single L-point ALE weight vector after the ALE has processed N data points, where $L \ll N$. The detection statistic is defined as

$$q_w = u_w^2 + v_w^2, \tag{36}$$

where

$$u_w = \sum_{\ell=0}^{L-1} w_\ell(k) \cos \omega_0 \ell$$

and

$$v_w = \sum_{\ell=0}^{L-1} w_\ell(k) \sin \omega_0 \ell \quad . \tag{37}$$

It is assumed (ref. 26) that $w_\ell(k)$ is given by (16) and that the weight variance (equal under H_0 and H_1) is given by (8). Therefore P_{FA} and P_D can be obtained from integrals of the form (ref. 26):

$$P_{FA} = \int_{z=T_0}^{\infty} \chi_2^2 (z)\, dz \tag{38}$$

and

$$P_D = \int_{z=T_0}^{\infty} \chi_2^{2'} (z \mid \alpha_w)\, dz \quad , \tag{39}$$

where $\alpha_w = 2_a^2(k)/\sigma_w^2$, and σ_w^2 is the weight variance defined by (8); i.e., $\sigma_w^2 = \mu \xi_{min} L$. (Note that the lower limits of the P_D and P_{FA} integrals are equal in this case.) These integrals (38,39) can also be evaluated using the nomograms in reference 38.

OPTIMAL DETECTION

The optimal likelihood ratio detector for a sinusoid of unknown amplitude and phase is shown in figure 3 (ref. 30). Since the frequency of the sinusoid ω_0 is a known priori, this optimal detection structure can be implemented using a DFT which transforms the input sampled data sequence to ensure that ω_0 is one of the DFT frequencies. The real and imaginary parts of the DFT are squared and summed to form the test statistic. The test statistic is formed from a coherent summation of the squared output over the entire observation interval. For the Gaussian white input noise sequence defined by (1), the resulting P_{FA} and P_D are

$$P_{FA} = \int_{z=\beta_0}^{\infty} \chi_2^2(z)\, dz \tag{40}$$

and

$$P_D = \int_{z=\beta_0}^{\infty} \chi_2^{2'}(z \mid N\,SNR)\, dz \quad , \tag{41}$$

where N is the total number of points in the observation interval.

DETECTION STATISTICS FOR INCOHERENTLY AVERAGED DFT PROCESSOR

In applications where the total time duration of the signal N is unknown a priori, or in cases where the input time-bandwidth product is large, it may not be practical to match the length of the coherent summation to N. In such cases, the suboptimal structure shown in figure 3(b) is often used. In this case the N-length input sequence is divided into M blocks of K points each, and a coherent K-point DFT is formed for each block. The block DFTs are then averaged, forming the detection statistic u (normalized to unity variance), which is the magnitude square of the ω_0 component. Under H_0 the detection statistic u is a chi-squared density function with 2M degrees of freedom (ref. 30,38). Thus

$$P_{FA} = \int_{\mu=\beta_0}^{\infty} \chi_{2M}^2(u)du \quad . \tag{42}$$

Under H_1 the detection statistic u is a noncentral chi-squared density function with 2M degrees of freedom and noncentrality parameter $\alpha_I = N(SNR)$ (ref. 38). Since the statistical variance on u is not dependent upon signal presence or absence, the threshold under H_1 is also equal to β_0. Thus

$$P_D = \int_{\mu=\beta_0}^{\infty} \chi_{2M}^{2'}(u \mid \alpha_I)du \quad . \tag{43}$$

The quantities β_0 and P_D may be evaluated using the nomograms presented in reference 38. Note that the performance of the quadratic detector for this case, as shown in figure 6 below, is closely approximated by the ROC curves developed by Robertson (ref. 40). An extensive discussion of the performance of this class of detectors is presented in reference 30.

PERFORMANCE ANALYSIS

The detection performance of the adaptive implementations and the conventional DFT processor of the previous section will be compared on the basis of ROC analysis. A value of P_{FA} is specified and held constant for a set of hypotheses tests, while the input signal strength is varied. The results are sets of curves which give P_D as a function of input SNR for different processor configurations.

For the ALE detectors there is a fundamental trade-off in the selection of μ between the midadjustment noise (8) and the convergence time (17). In the output detector, for a given P_{FA}, the probability of detection is an increasing function of α and a decreasing function of σ_0/σ_1 (26,27). Furthermore, from (34,35), it can be seen that α and σ_0/σ_1 are monotonic functions (increasing and decreasing respectively) of $a^2(N)/\mu$, where N is the length of the data sequence. Similarly, Reeves (ref. 39) has shown that the detection performance of the weight implementation is a function of $a^2(N)/\mu$. Thus, maximizing detectability at time N with respect to μ is equivalent to maximizing $a^2(N)/\mu$ and yields the following relationship between μ_{op} and N for both adaptive implementations:

$$\mu_{op} = \frac{1.25643}{N\,2v^2\left(1+\frac{L}{2}\,SNR\right)}\,,\quad N \gg L. \tag{44}$$

It follows from (17) that optimal detection is obtained at $a(k) = 0.715a^*$, indicating that the ALE weight vector has reached 71.5 percent of its steady-state value.

Detection performance is not critically dependent on the choice of μ when μ is close to μ_{op}. This is illustrated in figure 4, where the SNR at which $P_D = 0.5$ is plotted as a function of μ for $P_{FA} = 10^{-4}$.

Figure 5 displays P_D versus input SNR for the case K = L = 1024 and an input data sequence of N = 100L points. The ROC curves for the ALE implementation are compared with those of a coherent DFT of length N and an incoherently averaged DFT (IAD) processor which averages the power spectra of 100 K-point DFTs. The performance of the two adaptive detectors is nearly equivalent (within 0.5 dB) to that of the IAD process in the vicinity of $P_D = 0.50$.

Figure 6 shows the effect of the DFT length on detection. The primary difference from figure 5 is a rise in the detectable SNR levels reflecting the loss in coherent gain, $10 \log K_1/K_2$, caused by the decreased resolution. On the other hand, changing the ratio N/L affects the incoherent gain, producing an approximate loss of $5 \log [(N_1L_2)/(N_2L_1)]$ (compare figures 5 and 7).

Note that the value of μ was optimized in the above cases. The relative behavior of the IAD and the two adaptive detector implementations also remained similar when the DFT and ALE lengths were shortened to K = L = 128.

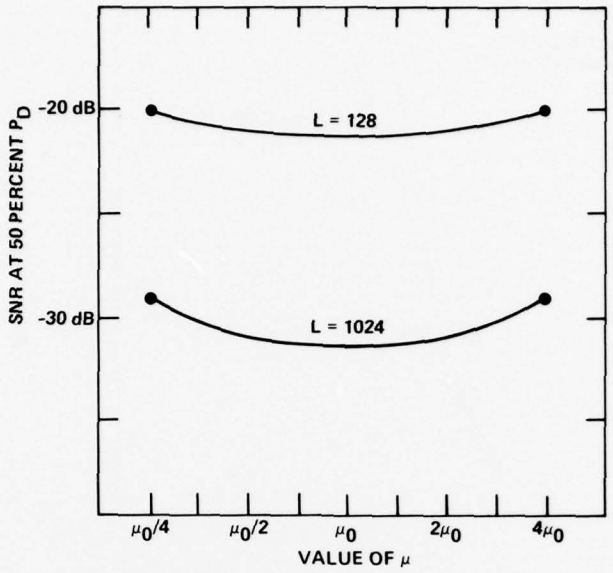

Figure 4. Sensitivity in detection performance to choice of adaptive time constant for ALE weight and output detectors: SNR versus μ for P_D = 50 percent, $P_{FA} = 10^{-4}$, K = L and N = 100L. Under these parameters the ALE weights and ALE output differed by less than 0.2 dB, and thus a single curve appears for both detectors.

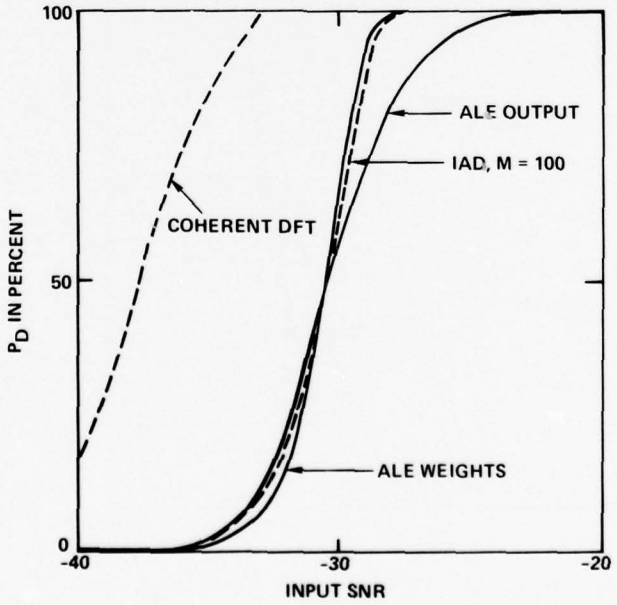

Figure 5. ROC curves for $P_{FA} = 10^{-4}$, N = 102400, K = L = 1024, $\mu\xi$ min = 4.1×10^{-6}; μ is optimal at SNR = 30.1 dB ($P_D \cong 50$ percent).

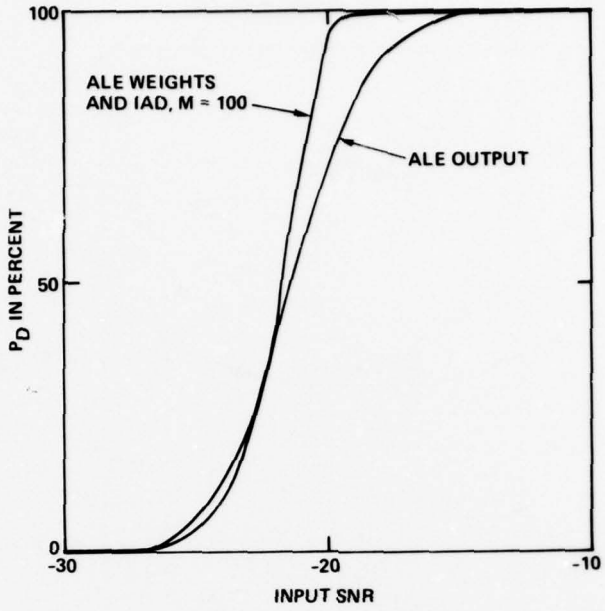

Figure 6. ROC curves for $P_{FA} = 10^{-4}$, N = 12800, K = L = 128, $\mu\xi$ min= 3.3×10^{-5}; μ is optimal at -21.2 dB ($P_D \cong 50$ percent). The ALE weights and IAD coincided within the accuracy of the figure.

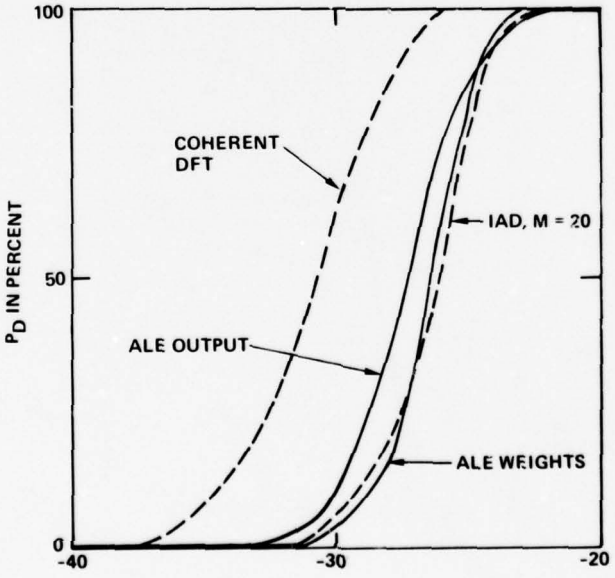

Figure 7. ROC curves for $P_{FA} = 10^{-4}$, N = 20480, K = L = 1024, $\mu\xi_{min} = 1.54 \times 10^{-5}$; μ is optimal at SNR = 27.1 dB ($P_D \cong 50$ percent).

Figure 8 illustrates the effects of changing K/L for the ALE output device. ALE detection performance is a nonlinear function of K/L as indicated by (34) and (35). In figure 8, L is fixed at 1024, and K is variable from 64 to 16,192. The parameter μ is optimized at each SNR using (44). A variation of between 3 log (K/L) and 5 log (K/L) is indicated as K/L is varied by factors of 4.

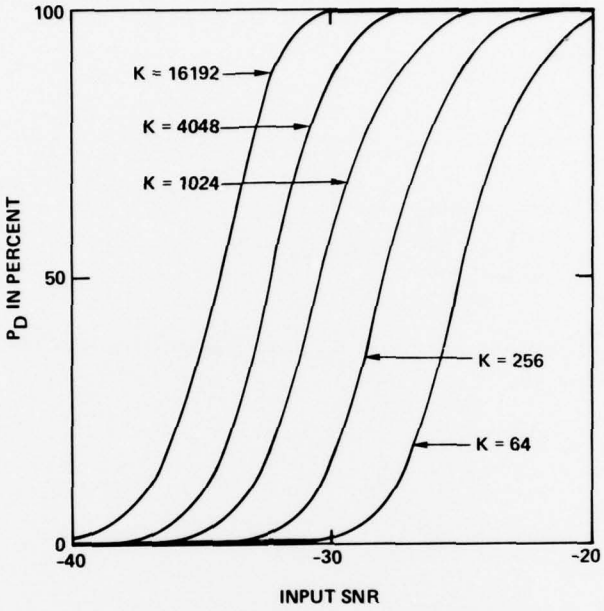

Figure 8. ROC curves for ALE output detector for fixed filter length L = 1024 and varying DFT length K with $P_{FA} = 10^{-4}$, $\mu\xi_{min} = 4.1 \times 10^{-6}$, and N = 102400; μ is optimal at SNR = 30.1 dB.

SUMMARY

This paper has examined the detection properties of two adaptive detectors for the SKEP probelm. ROC curves were computed for the two adaptive implementations (an L-point ALE followed by a K-point DFT of the filter weight vector or output) and compared to those of an optimal DFT of length N and a K-point DFT with coherent averaging. The effects of the parameters K and L and of the data sequence length N were discussed. It was found that, when K = L, the two adaptive detector implementations performed similarly to an incoherently averaged DFT, provided that the feedback constant μ was optimized for a given N, L, and SNR. The sensitivity of detection performance to the choice of the adaptive time constant for a given observation interval was discussed. Finally the effect of a resolution mismatch between the ALE and the DFT was investigated.

The results obtained in the paper are based on the assumptions that the ALE output noise statistics are Gaussian and that the magnitude-square transform of the ALE output has a chi-square density with two degrees of freedom. Future work will concentrate on defining these densities experimentally and obtaining experimental verification of the analytical ROC curves presented here. It will also include the effects of post detection integration.

APPENDIX

The purpose of this appendix is to calculate the means and variances of the two variables u and v appearing in equation (23).

Two expressions,

$$G_M = G_1(\omega, b) = \sum_{k=0}^{M-1} \cos(2\omega k + b) \tag{A.1}$$

and

$$G'_M = \frac{1}{2}\frac{dG}{d\omega}\left(\omega, b + \frac{\pi}{2}\right) = \sum_{k=0}^{M-1} k \cos(2\omega k + b) \ ,$$

will occur frequently throughout the calculations. These expressions may be evaluated (using standard identies) through

$$G_M = \frac{\sin M\omega}{\sin \omega} \sin(\omega(M-1) + b) \ , \tag{A.2}$$

and are bounded (ref. 33) by

$$|G_M| << M$$

$$|G'_M| << M^2 \tag{A.3}$$

under the condition

$$\frac{\pi}{M} << \omega << \pi - \frac{\pi}{M} \ . \tag{A.4}$$

Throughout the remainder of the appendix (unless otherwise stated) we shall assume that (A.4) is satisfied where

$$M = \min(L,K) \ . \tag{A.5}$$

In addition, we will assume that the delay is 1:

$$\Delta = 1 \tag{A.6}$$

Two other identities will be useful:

$$\cos\omega(\ell - k)\sin\omega\ell\cos\omega k = \frac{1}{4}[\sin 2\omega(\ell - k) + \sin 2\omega\ell + \sin 2\omega k] \tag{A.7a}$$

and

$$\cos\omega(\ell - k)\cos\omega\ell\cos\omega k = \frac{1}{4}[1 + \cos 2\omega(\ell - k) + \cos 2\omega\ell + \cos 2\omega k] \ , \tag{A.7b}$$

which may easily be verified by substituting exponentials; e.g., $\cos\omega\ell = \frac{1}{2}(e^{i\omega\ell} + e^{-i\omega\ell})$, etc.

CALCULATION OF MEANS

$$E(u) = \sum_{k=0}^{K-1} \sum_{\ell=0}^{L-1} E[W_\ell(k)\, X(k - \ell - 1) \cos \omega k]$$

$$= A \sum_{k,\ell} W_\ell^* \sin(\omega(k - \ell - 1) + \theta) \cos \omega k$$

$$= \frac{2a^*A}{L} \sum_{k,\ell} \sin(\omega(k - \ell - 1) + \theta) \cos \omega(\ell + 1) \cos \omega k$$

$$= \frac{2^*A}{L} \sum_{k,\ell} \sin\, [(\omega(k - \ell - 1) \cos \theta + \cos \omega(k - \ell - 1) \sin \theta]$$

$$[\cos(\omega(\ell + 1)) \cos \omega k] \quad .$$

Use of (A.7) and the identity $\sin(\omega n + \theta) = \sin \omega n \cos \theta + \cos \omega n \sin \theta$ yields

$$E(u) = \frac{2a^*A}{L} \frac{1}{4} \sum_{k,\ell} [\sin \theta + \sin(2\omega(k - \ell - 1) + \theta) + \sin(2\omega k + \theta) + \sin(2\omega\ell + \theta]. \tag{A.8}$$

Then, from (A.3),

$$E(u) = \frac{a^*A}{2L} \sum_{\ell=0}^{L-1} (K \sin \theta + \text{terms} << K) \cong \frac{a^*AKL}{2L} \sin \theta \quad . \tag{A.9}$$

Similarly

$$E(v) \cong \frac{a^*AK}{2} \cos \theta \quad . \tag{A.10}$$

More exact expressions may be found in reference 37.

CALCULATION OF σ_u^2 AND σ_v^2

The variance of u is given by (23):

$$\sigma_u^2 = E(u^2) - E(u)^2$$

$$= \sum_{\ell,k=0}^{K-1} \gamma_r(\ell - k) \cos \omega k \cos \omega\ell \quad , \tag{A.11}$$

where

$$\gamma_r(m) = E\{(r(k \mid \theta)\, r(k+m \mid \theta)\} - E[r(k \mid \theta)]\; E[r(k+m \mid \theta)] \quad . \tag{A.12}$$

It follows, from the approximate independence of w_j and X_j (5), that for $\Delta = 1$

$$E(r(k \mid \theta)) = E\left(\sum_{\ell=0}^{L-1} w_\ell(k)\, x(k-\ell)\right)$$

$$= \sum_{\ell}^{L-1} E[(w_\ell(k)]\; E[A \sin((k-\ell-1)\,\omega + \theta) + n(k-\ell-1)]$$

$$= \sum_{\ell}^{L-1} w_\ell^*\, A \sin(\omega(k-\ell-1)+\theta) \quad . \tag{A.13}$$

Now let

$$\phi(m) = E[r(k \mid \theta)\, r(k+m \mid \theta)]$$

$$= E \sum_{j=0}^{L-1} \sum_{i=0}^{L-1} [w_j(k)\, w_i(k+m)]\,[A \sin \omega(k-j-1)+\theta] + [n(k-j-\Delta)]$$

$$\cdot\, [A \sin \omega(k+m-i-1)+\theta] + [n(k+m-i-1)] \quad . \tag{A.14}$$

Again, since the weight vectors w_j and the white noise input n are essentially uncorrelated, and since $E(n) = 0$, most of the terms in (A.14) vanish. Two terms remain

$$\phi(m) = \phi_1 + \phi_2 \quad , \tag{A.15}$$

where

$$\phi_1 = E\left[\sum_{i,j,=0}^{L-1} [w_j(k)\, w_i(k+m)]\; A^2 \sin(\omega(k-j-1)+\theta) \sin(\omega(k+m-i-1)+\theta)\right]; \tag{A.16}$$

$$\phi_2 = E\left[\sum_{i,j=0}^{L-1} w_j(k)\, w_i(k+m)\, n(k-j-1)\, n(k+m-i-1)\right] \quad . \tag{A.17}$$

In reference 36 it is shown that the misadjustment noise $V_j(k)$ is highly correlated in time and consequently (compare (8)) that

$$E(V_j(k)\, V_i(k+m)) = \mu\xi^2 \delta(i-j) \quad . \tag{A.18}$$

This and (7) yield

$$E[(w_j(k)\, w_i(k+m)] = w_j^*\, w_i^* + \delta(i-j)\,\mu\xi^2 \quad . \tag{A.19}$$

We now calculate ϕ_1. Substituting (A.13) and (A.19) in (A.16), we have

$$\phi_1 = A^2\mu\xi^2 \left[\sum_{j=0}^{L-1} \sin(\omega(k-j-1)+\theta)\, \sin(\omega(k-j+m-1)+\theta) + E(r(k\,|\,\theta))\, E(r(k+m\,|\,\theta)) \right] . \tag{A.20}$$

Using the identities

$$\sin a \sin(a+b) = \frac{\cos b}{2} - \frac{\cos(2a+b)}{2} \tag{A.21}$$

and (A.1) and (A.3) we obtain

$$\phi_1 = \frac{A\mu\xi^2}{2} \cos \omega m (L + \text{terms} << L) + E(r(k\,|\,\theta))\, E(r(k+m)\,\theta))$$

$$\cong \frac{A\mu\xi^2}{2} L \cos \omega m + E(r(k\,|\,\theta))\, E(r(k+m)\,\theta)) \quad . \tag{A.22}$$

Since the input noise n is assumed to be white, (A.17) and (A.19) yield

$$\phi_2 = \sum_{k,\ell=0}^{L-1} (w_k^*\, w_\ell^* + \delta(k-\ell)\,\mu\xi^2)\, \delta(m-\ell+k)\, v^2 \tag{A.23}$$

$$= \left.\begin{array}{l} \displaystyle\sum_{k=0}^{L-1-|m|} w_k^*\, w_{k+|m|}^* v^2 + L\,\delta(m) v^2 \mu\xi^2 \\ 0 \end{array}\right\} \begin{array}{l} |m| < L \\ |m| \geqslant L \end{array} . \tag{A.24}$$

From (11) and (A.21) we have

$$w_k^*\, w_{k+|m|}^* = \frac{4a^{*2}}{L^2} (\cos \omega(k+1) \cos \omega(k+m+1))$$

$$= \frac{2a^{*2}}{L^2} (\cos \omega m + \cos \omega(2k+m+2)) \quad . \tag{A.25}$$

Substituting (A.25) into (A.24) and using the identity (A.2) we obtain

$$\phi_2 = \left.\begin{array}{l} \tilde{\phi}_2 \\ 0 \end{array}\right\} \begin{array}{l} |m| < L \\ |m| \geqslant L \end{array} , \tag{A.26}$$

where

$$\tilde{\phi}_2 = \frac{2a^{*2}\upsilon^2}{L^2}\left[(L - |m|)\cos\omega_0 m + \frac{\cos\omega_0(L+1)}{\sin\omega_0}\sin\omega_0(L - |m|)\right] . \quad (A.27)$$

Combining (A.12), (A.15), (A.22), and (A.27) we finally obtain

$$\left.\begin{array}{ll} \gamma(m) = \gamma_1 + \gamma_2 + \gamma_3 + \gamma_4 & |m| < L \\ \gamma_2 & |m| \geq L \end{array}\right\} , \quad (A.28)$$

where

$$\gamma_1 = \mu\xi^2\upsilon^2\delta(m) \quad (A.29)$$

$$\gamma_2 = \frac{A^2\mu\xi^2 L}{2}\cos\omega m \quad (A.30)$$

$$\gamma_3 = \frac{2a^*\upsilon^2}{L^2}(L - |m|)\cos\omega m \quad (A.31)$$

$$\gamma_4 = \frac{2a^*\upsilon^2}{L^2}\,\frac{\cos\omega(L+1)}{\sin\omega}\sin\omega(L - |m|) . \quad (A.32)$$

Let

$$a = \mu\xi^2\upsilon L \quad , \quad b = \frac{\mu\xi^2 L A^2}{2}$$

$$c = \frac{2a^2\upsilon^2}{L^2} \quad , \quad d = \frac{\cos\omega(L+1)}{\sin\omega} \quad (A.33)$$

Then substitution of (A.28) in (A.11) yields four terms, each containing a double sum over $\ell,k=0, \ldots, K-1$ and three of the terms restricted to $|k-\ell| \leq L-1$. Thus

$$\sigma_u^2 = \sigma_1^2 + \sigma_2^2 + \sigma_3^2 + \sigma_4^2 , \quad (A.34)$$

where

$$\sigma_1^2 = \sum_{|\ell-k|<L} a\delta(\ell - k)\cos\omega k\cos\omega\ell , \quad (A.35)$$

$$\sigma_2^2 = \sum_{\ell,k}^{K-1} b\cos(\ell - k)\cos\omega k\cos\omega\ell , \quad (A.36)$$

$$\sigma_3^2 = \sum_{|\ell-k|<L} c\,(L - |\,\ell - k\,|)\cos\omega(\ell - k)\cos\omega k\cos\omega\ell \quad , \tag{A.37}$$

$$\sigma_4^2 = \sum_{|\ell-k|<L} cd\,\sin\omega(\ell - k)\cos\omega k\cos\omega\ell \quad . \tag{A.38}$$

If we make the substitution $n = \ell - k$, then

$$\sum_{|\ell-k|<L} \rightarrow \sum_{n-1-M}^{M-1} \sum_{k=0}^{K-|n|-1} \quad ,$$

$$\sum_{\ell,k} \rightarrow \sum_{n\ell=0}^{K-1} \sum_{k=0}^{K-1} \quad ,$$

where $M = \min(L,K)$ as in (A.5).

$$\sigma_1^2 = a \sum_{1-M}^{M-1} \sum_{k=0}^{K-|n|-1} \delta(n)\cos\omega k\cos\omega(n + k) \quad ,$$

$$= a \sum_{k=0}^{K-1} (\cos\omega k)^2 \quad .$$

But $(\cos\omega k)^2 = \dfrac{1 + \cos 2\omega k}{2}$, so that by (A.3)

$$\sigma_1^2 \cong \frac{aK}{2} \quad . \tag{A.39}$$

We now calculate σ_2^2:

$$\sigma_2^2 = \sum_{\ell=0}^{K-1} \sum_{k=0}^{K-1} b\cos\omega(\ell-k)\cos\omega\ell\cos(\omega k)$$

$$= \sum_{\ell=0}^{K-1} \sum_{k=0}^{K-1} \frac{b}{4}\,[1 + \cos 2\omega\ell + \cos\omega k + \cos 2\omega(\ell - k)] \quad .$$

Under (A.3)

$$\left|\sum_{\ell=0}^{K-1} \sum_{\ell=0}^{K-1} \cos 2\omega(\ell - k)\right| \leqslant \sum_{\ell=0}^{K-1} \left|\sum_{k=0}^{K-1} \cos\omega(\ell - k)\right| << K \cdot K = K^2 \quad . \tag{A.40}$$

Similar expressions for the remaining terms yield

$$\sigma_2^2 = \frac{b}{4} K^2 + \text{terms} << K^2$$

$$\cong \frac{b}{4} K^2 \quad . \tag{A.41}$$

To calculate σ_3^2:

$$\sigma_3^2 = \sum_{n=-M+1}^{M-1} \sum_{k=0}^{K-|n|-1} c(L - |n|) \cos \omega n \cos \omega k \cos \omega(k + n)$$

$$= 2 \sum_{n=0}^{M-1} \sum_{k=0}^{K-n-1} c(L - n) \cos \omega n \cos \omega k \cos \omega(k+n) - cL \sum_{k=0}^{K-1} \cos^2 \omega k \tag{A.42}$$

We note using (A.1) to (A.3) that

$$\left| \sum_{k=0}^{K-1} \cos^2 \omega k \right| << K$$

We further note that

$$2 \left| \sum_{n=0}^{M-1} \sum_{k=0}^{K-n-1} L \cos 2\omega(k + n) \right| < 2ML \left| \sum_{k=0}^{K-n-1} \cos \alpha\omega(k + n) \right| << 2MLK \tag{A.43}$$

and that

$$2 \left| \sum_{n=0}^{M-1} \sum_{k=0}^{k-n-1} n \cos 2\omega(k + n) \right|$$

$$= 2 \left| \sum_{n=0}^{M} \sum_{k=0}^{K-n-1} (n \cos 2\omega k \cos 2\omega n - n \sin 2wk \sin 2\omega n \right| << 4M^2K < 4MKL \quad .$$

(A.44)

Similar expressions hold for cos 2ωn and cos 2ωk. The substitution of identity (A.7b) and (A.42) and the use of approximations (A.43), (A.44), etc., yield

$$\sigma_3^2 = 2 \sum_{n=0}^{M-1} \sum_{k=0}^{K-n-1} \frac{c}{4} (L - n) + \frac{c}{4} (\text{terms} << MLK). \tag{A.45}$$

Also

$$\sum_{n=0}^{M-1} \sum_{k=0}^{K-n-1} L = L \sum_{n=0}^{M-1} (K - n) = L\,MK - \frac{LM^2}{2} + (\text{terms} << LMK) \qquad (A.46)$$

and

$$\sum_{n=0}^{M-1} \sum_{k=0}^{K-n-1} n = \sum_{n=0}^{M-1} (K - n)n = \frac{M^2K}{2} - \frac{M^3}{3} + (\text{terms} << LMK). \qquad (A.47)$$

Combining (A.45) through (A.47), we have

$$\sigma_3^2 = \frac{c}{4}\left[2KLM - LM^2 - KM^2 + \frac{2}{3}M^3 + \text{terms} << LMK\right]$$

$$= \begin{cases} c\left[\frac{K^2L}{4} - \frac{K^3}{12} + \text{terms} << K^2L\right], & K \leqslant L \\ c\left[\frac{L^2K}{4} - \frac{L^3}{12} + \text{terms} << L^2K\right], & K \geqslant L \end{cases}$$

$$\cong \begin{cases} \frac{c}{4} D \text{ where } D = \frac{K^2L}{4} - \frac{K^3}{12}, & K \leqslant L \\ \frac{L^2K}{4} - \frac{L^3}{12}, & K \geqslant L \end{cases} . \qquad (A.48)$$

We conclude with σ_4^2:

$$\sigma_4^2 = \sum_{n=-M+1}^{M-1} \sum_{k=0}^{K-|n|-1} cd \sin \omega n \cos \omega k \cos \omega(n + k) . \qquad (A.49)$$

From identity (A.7a) and approximations of the type of (A.40):

$$\sigma_4^2 << \frac{c}{4} d\,(\text{terms} << MK) . \qquad (A.50)$$

Since (A.4) implies that $d << L$,

$$\sigma_4^2 << \frac{c}{4} MKL ,$$

i.e.,

$$\sigma_4^2 << \sigma_3^2 . \qquad (A.51)$$

Finally, from (A.34), (A.39), (A.41), (A.48), and (A.51) we obtain

$$\sigma_u^2 \cong \frac{ak}{2} + \frac{bk^4}{4} + cD = \frac{\mu\xi^2 \upsilon^2 LK}{2} + \frac{\mu\xi^2 A^2 LK^2}{8} + 2\frac{a^{*2}\upsilon^2}{L^2} D , \qquad (A.52)$$

where

$$D = \begin{cases} \frac{K^2 L}{4} - \frac{K^3}{12} & , \ K \leqslant L \\ \frac{L^2 K}{4} - \frac{L^3}{12} & , \ K \geqslant L \ . \end{cases}$$

Since σ_u^2 is approximately independent of ω, we must have

$$\sigma_v^2 \cong \sigma_u^2 \tag{A.53}$$

CALCULATION OF σ_{uv}

$$\sigma_{uv} = \sum_{k=0}^{K-1} \sum_{\ell=0}^{K-1} \gamma_r(\ell - k) \cos \omega\ell \sin \omega k \ . \tag{A.54}$$

Substitution of (A.32) in (A.50) yields four terms

$$\sigma_{uv}^2 = \alpha_1 + \alpha_2 + \alpha_3 + \alpha_4$$

similar to (A.35) through (A.38) except that $\cos \omega k$ is replaced by $\sin \omega k$. The first term gives

$$\alpha_1 = \sum_{|\ell - k| < L} \alpha\delta(\ell - k) \cos \omega\ell \sin \omega k$$

$$= \frac{a}{2} \sum_{k=1}^{K-1} \sin 2\omega k \ , \ |\alpha_1| << \frac{a}{2} K \ . \tag{A.55}$$

The next two terms contain the expression

$$\cos \omega(\ell - k) \cos \omega\ell \sin \omega k = \frac{1}{4} [\sin 2\omega(\ell - k) + \sin 2\omega\ell + \sin 2\omega k] \ . \tag{A.56}$$

As in (A.40), (A.43), and (A.44)

$$\sum_{\ell,k} \left| (\sin 2w(\ell - k) \right| << K^2 \ ,$$

$$\left| \sum_{n=0}^{M-1} \sum_{k=0}^{K-n-1} (\sin 2\omega(k + n) \right| << MLK \ ,$$

and

$$\left| \sum_{n=0}^{M-1} \sum_{k=0}^{K-n-1} n \sin 2w(k+n) \right| << 2MLK \quad . \tag{A.57}$$

Similar expressions are valid for $\sin 2\omega\ell$ and $\sin 2\omega k$. Thus

$$\alpha_2 = \sum_{\ell,k} b \sin \omega(\ell - k) \sin \omega\ell \sin \omega k$$

$$= \frac{b}{4} (\text{terms} << K^2) \quad ; \tag{A.58}$$

$$\alpha_3 = \sum_{n=-M+1}^{M-1} \sum_{k=0}^{K-|n|-1} c\,(L - |n|) \cos \omega n \cos \omega(n+k) \sin \omega k$$

$$= \frac{c}{4} (\text{terms} << LMK) \quad ; \tag{A.59}$$

$$\alpha_4^2 = \sum_{n=-M+1}^{M-1} \sum_{k=0}^{K-|n|-1} c\,d \sin \omega n \cos \omega(n+k) \sin \omega k \quad . \tag{A.60}$$

Once again

$$\sin \omega n \cos \omega(n+k) \sin \omega k = \frac{1}{4} [1 + \cos 2\omega(n+k) - \cos 2\omega n - \cos 2\omega k] \quad .$$

Thus

$$|\alpha_4| \leqslant \frac{cd}{4} (2MK + \text{terms} << MK)$$

$$<< \frac{c}{4} (LMK) \quad . \tag{A.61}$$

Comparing (A.55), (A.58), (A.59), and (A.61) with σ_1^2, σ_2^2, σ_3^2, and σ_4^2 we see that

$$|\sigma_{uv}| << \sigma_u^2 \quad .$$

REFERENCES

1. J. T. Rickard and G. M. Dillard, "Adaptive Detection Algorithms for Multiple Target Situations," IEEE Trans. on Aerospace and Electronic Systems, vol. AES-13, p. 338, 1977.

2. J. T. Rickard and G. M. Dillard, "Adaptive Detection Algorithms for Multiple-Target Spectral Data," Proc. of the 1977 IEEE Conference on Decision and Control, p. 515, 1977.

3. D. Gupta, J. Beteline, T. Curry, and J. Frances, "An Adaptive Threshold System for Nonstationary Noise Background," IEEE Trans. on Aerospace and Electronic Systems, vol. AES-13, p. 11, 1977.

4. G. Dillard, "Mean Level Detection of Nonfluctuating Signals," IEEE Trans. on Aerospace and Electronic Systems, vol. AES-10, p. 795, 1974.

5. R. Nitzberg, "Constant False Alarm Rate Processors for Locally Non-Stationary Clutter," IEEE Trans. on Aerospace and Electronic Systems, vol. AES-9, p. 399, 1977.

6. R. Nitzberg, "Constant False Alarm Rate Signal Processors for Several Types of Interference," IEEE Trans. on Aerospace and Electronic Systems, vol. AES-8, p. 27, 1972.

7. B. Steeson, "Detection Performance on a Mean Level Threshold," IEEE Trans. on Aerospace and Electronic Systems, vol. AES-4, p. 529, 1968.

8. E. Baxa and L. Nolte, "Adaptive Signal Detection with Finite Memory," IEEE Trans. on Systems, Man, and Cybernetics, vol. 2, p. 42, 1972.

9. H. Groginsky, L. Wilson, and D. Middleton, "Adaptive Detection of Signals in Noise," IEEE Trans on Information Theory, vol. IT-12, p. 377, 1966.

10. H. Scudder III, "Adaptive Communications Receivers," IEEE Trans on Information Theory, vol. IT-11, p. 167, 1965.

11. N. Abramson and D. Braverman, "Learning to Recognize Patterns in a Random Environment," Trans. IRE, vol. IT-8, p. 58, 1962.

12. E. Glaser, "Signal Detection by Adaptive Filters," Trans. IRE, vol. IT-7, p. 87, 1961.

13. M. Woinsky, "Nonparametric Detection using Spectral Data," IEEE Trans. on Information Theory, vol. IT-18, pp. 110–118, 1972.

14. C. Helstrom, Statistical Theory of Signal Detection, Pergamon Press, Oxford, 1975.

15. J. Makhoul, "Linear Prediction: A Tutorial Review," Proc. IEEE, vol. 63, p. 561, 1975.

16. L. Griffiths, "Rapid Measurement of Digital Instantaneous Frequency," IEEE Trans. on Acoustics, Speech, and Signal Processing, vol. ASSP-23, p. 209, 1975.

17. B. Widrow et al., "Adaptive Noise Cancelling: Principles and Applications," Proc. IEEE, vol. 63, p. 1962, 1975.

18. D. Morgan and S. Craig, "Real Time Linear Prediction using the Least Mean Squares Adaptive Algorithm," IEEE Trans. on Acoustics, Speech, and Signal Processing, vol. ASSP-24, p. 494, 1976.

19. R. Keeler and L. Griffiths, "Acoustic Doppler Extraction by Adaptive Linear Prediction Filtering," Journal of the Acoustical Society of America, vol. 61, p. 1812, 1977

20. L. J. Griffiths, R. R. Smolka, and L. D. Trembly, "Adaptive Deconvolution: A New Technique for Processing Time Varying Seismic Data," Geophysics, vol. 42, p. 742, 1977.

21. J. Treichler, "The Spectral Line Enhancer – The Concept, an Implementation and an Application," PhD Dissertation, Dept. of Electrical Engineering, Stanford University, 1977.

22. D. W. Tufts, L. J. Griffiths, B. Widrow, J. Glover, J. McCool, and J. Treichler, "Adaptive Line Enhancement and Spectral Analysis," Proc. IEEE, vol. 65, p. 169, 1977.

23. J. Zeidler, E. Satorius, D. Chabries, and H. Wexler, "Adaptive Enhancement of Multiple Sinusoids in Uncorrelated Noise," IEEE Trans. on Acoustics, Speech, and Signal Processing, vol. ASSP-26, p. 240, 1978.

24. W. S. Burdic, "Detection of Narrowband Signals using Time Domain Adaptive Filters," to be published in IEEE Trans. on Aerospace and Electronics.

25. N. Ahmed, D. Hummels, M. Uhl and D. Soldan, "A Short Term Regression Algorithm," Proc. 1978 International Conference on Acoustics, Speech, and Signal Processing (ICASSP), p. 123.

26. L. R. Rabiner, R. E. Crochiere, J. B. Allen, "Comparisons of System Identification Methods in the Presence of High Noise Levels and Bandlimited Inputs," Proc. 1978 ICASSP, p. 183.

27. J. Makhoul and R. Viswanathan, "Adaptive Lattice Methods for Linear Prediction," Proc. 1978 ICASSP, p. 83.

28. S. T. Alexander, E. H. Satorius, and J. R. Zeidler, "Linear Prediction and Maximum Entropy Spectral Analysis of Finite Bandwidth Signals in Noise," Proc. 1978 ICASSP, p. 188.

29. M. Sanbur, "LMS Adaptive Filtering for Enhancing the Quality of Noisy Speech," Proc. 1978 ICASSP, p. 610.

30. A. D. Whalen, Detection of Signals in Noise, Academic Press, New York, 1971.

31. R. A. Roberts, "On the Detection of a Signal Known Except for Phase," IEEE Trans. on Information Theory, vol. IT-11, p. 76, 1965.

32. B. Widrow, "Adaptive Filters," in Aspects of Network and System Theory, R. Kalman and N. DeClaris, Eds., New York: Holt, Rinehart, and Winston, Inc., 1971.

33. M. Sondhi and D. Mitra, "New Results on the Performance of a Well-Known Class of Adaptive Filters," Proc. IEEE, vol. 64, p. 1583, 1976.

34. A. Weiss and D. Mitra, "Some Mathematical Results on the Effects on Digital Adaptive Filters of Impelmentation Errors and Noise, Proc. 1978 ICASSP, p. 113.

35. J. T. Rickard and J. R. Zeidler, "Second Order Statistics of the Adaptive Line Enhancer," Naval Ocean Systems Center, Technical Report 202, January 1978; to be published in IEEE Trans. on Acoustics, Speech, and Signal Processing.

36. L. J. Griffiths, J. Keeler, and R. Medaugh, "Detection and Convergence Results Relating to the Performance of an Adaptive Line Enhancer," Naval Undersea Center, Technical Note 1831, December 1976.

37. S. T. Alexander, "The ALE Output Covariance Function for a Sinusoid in Uncorrelated Noise," Naval Ocean Systems Center, Technical Report 162, August 1977.

38. H. Urkowitz, "Energy Detection of Unknown Deterministic Signals," Proc. IEEE, vol. 55, April 1967.

39. P. M. Reeves, "Detection of Narrowband Signals using Time Domain Adaptive Filters," Naval Ocean Systems Center, Technical Report 180, November 1977.

40. G. H. Robertson, "Operating Characteristics for a Linear Detector of CW Signals in Narrowband Gaussian Noise," Bell Systems Technical Journal, vol. 46, p. 755, 1967.